Polymer 42 (2001) 8019–8023

polymer

www.elsevier.nl/locate/polymer

Computational studies of the Brookhart's type catalysts for ethylene polymerization. 1. Effect of the active site conformations on the catalyst activities

J. Ramos[a], V. Cruz[b], A. Muñoz-Escalona[c], J. Martínez-Salazar[a,*]

[a]*GIDEM, Instituto de Estructura de la Materia, CSIC, Serrano 113-bis-119-121-123, 28006 Madrid, Spain*
[b]*CTI, CSIC Pinar 19, 28006 Madrid, Spain*
[c]*Repsol I + D, Embajadores 183, 28045 Madrid, Spain*

Received 20 March 2001; received in revised form 17 April 2001; accepted 1 May 2001

Abstract

DFT calculations have been carried out on the cationic species for the two different Brookhart's catalyst systems: $[\{ArN{=}CH{-}HC{=}NAr\}NiR'']^+$ (**3a**) and $[\{ArN{=}CMe{-}MeC{=}NAr\}NiR'']^+$ (**3b**) (where $Ar = \{2,6\text{-}C_6H_3(Me)_2\}$ and $R'' = Me$). These calculations reveal that the conformation of aryl groups attached to nitrogen atoms could provide a suitable explanation for the large experimental differences found in the ethylene polymerization activity. © 2001 Elsevier Science Ltd. All rights reserved.

Keywords: Poly(ethylene); Homogeneous catalysis; DFT calculations

1. Introduction

Diimine nickel(II) complexes have recently been used as catalysts for α-olefin polymerization by Brookhart's group [1,2] and have emerged as an alternative to traditional heterogeneous and homogeneous Ziegler–Natta catalysts. The general structure of the diimine Ni(II) catalysts is depicted in Scheme 1. Theoretical polymerization mechanism studies on nickel-based catalysts have been performed on model [3–7] or real systems [7–11] (see **1** and **2** in Scheme 1). The Cossee–Arlman [12] and Brookhart–Green [13] mechanisms are the most accepted for olefin polymerization by transition metal catalysts. According to these mechanisms, the first step involves the ethylene coordination into the cationic metal alkyl species, which has been suggested to be the active species between subsequent monomer insertions.

An interesting effect on the catalyst activity involving the pendant groups R' and R has been experimentally observed [1]. When $R' = Me$, the catalyst activity is about 4–5 times greater than when $R' = H$ under the same experimental conditions (1800 versus 400 kg of PE $(mol\ Ni)^{-1}\ h^{-1}$).

During the course of previous unpublished work, we noticed that the aryl rings bonded to the diimine N atoms could rotate around the *N*-aryl bond to reach more stable conformations via conjugation and agostic effects.

Previous published theoretical work has studied similar systems at the IMOMM (QM/MM) level [7–11]. In this framework, the aryl groups were only included as part of the molecular mechanics (MM) calculations. Thus, the possible electronic effects of these aryl groups (such as agostic interaction between a hydrogen atom belonging to any of the substituents attached to the phenyl groups and the metal atom, see below) cannot be suitably described by the IMOMM methods. We suggest that, for some cases, it would be necessary to include all atoms forming the real system in the quantum mechanical simulation in order to describe such electronic effects.

The aim of the present work is to investigate how the different conformations of the 'floppy' aryl groups attached to the nitrogen atoms in the cationic complex could affect the activity of the catalyst as well as the relationship between these conformations and the experimental catalytic activities described above. Work concerning the ethylene insertion and the elimination reaction for the Brookhart's systems and other nickel catalysts will be reported in two forthcoming papers (Parts 2 and 3). A comparison between B3LYP and BP86 results for these catalysts will be published in Part 4.

---

* Corresponding author. Tel.: +34-91-561-68-00; fax: +34-91-564-55-57.

0032-3861/01/$ - see front matter © 2001 Elsevier Science Ltd. All rights reserved.
PII: S0032-3861(01)00320-2

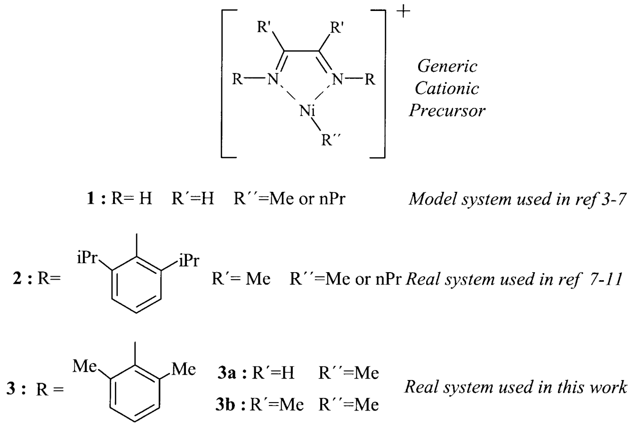

Scheme 1.

2. Computational methods

Geometries were optimized using the BP86 method included in ADF program [14] comprising local density approximation [15] but adding non-local corrections to exchange [16] and correlation [17]. Energies were obtained by applying the hybrid method B3LYP using the LANL2DZ basis set implemented in the GAUSSIAN 98 software [18]. It is well known that BP86 methods overestimate some weak interactions, as ligand–metal and agostic interactions with respect to B3LYP and higher level models [11]. Geometries obtained with the BP86 functionals are quite acceptable but energies are less reliable than the values obtained with B3LYP. On the other hand, B3LYP is computationally more demanding than BP86. These are the reasons why we have not used the B3LYP method for the geometry optimizations. Musaev et al. [11] showed that the energies calculated at the B3LYP level on BP86-optimized geometries are accurate enough as compared to higher levels of theory. We have been performing some calculations on similar organometallic compounds using BP86//BP86, B3LYP//BP86 and B3LYP//B3LYP models. The B3LYP//BP86 and the B3LYP//B3LYP energies found are very similar (differences lower than 2 kcal mol^{-1} were found). Also, the geometries obtained with the BP86//BP86 and the B3LYP//B3LYP methods are almost identical, with differences lower than 0.05 Å in distances and 1° in angles.

The approximate reaction paths were evaluated by a linear synchronous transit (LST) calculation.

3. Results and discussion

Several conformations of $[\{ArN{=}CR'{-}CR'{=}NAr\}NiR'']^+$ cationic complexes (where $Ar = \{2,6\text{-}C_6H_3(Me)_2\}$, $R' =$ H or Me and $R'' = Me$) have been studied, which differ on the relative position of the aryl groups with respect to the plane formed by the diimine ligand. The R$'$ substituents have a great influence in the stability of the different conformers, as will be shown below. The φ angle is monitored to quantify the position of the aryl groups as described by Ziegler et al. [8,9]. The definition of the φ angle is shown in Scheme 2. When φ is 90°, the aryl groups and the diimine–Ni ring are mutually perpendicular and when φ is 0° the two ligands are coplanar. It might be expected that conformations with φ angle close to 0° should hinder the monomer coordination into the active site catalyst reducing thus the polymerization activity (see below).

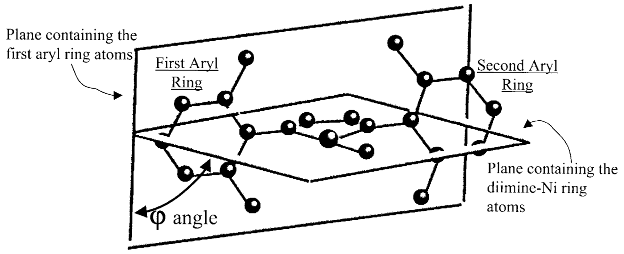

Scheme 2.

In the case of the complexes with hydrogen attached to diimine ligands (**3a** system), the three conformers found are shown in Fig. 1 along with the main geometrical parameters. Of the two aryl groups, only the first one can rotate because the rotation of the second one is hindered by the presence of methyl group. As a consequence, there exist three conformers depending on the first aryl ring φ angle (see Fig. 1). For conformer **3a.I**, the first aryl ring lies almost parallel to the Ni–diimine ligand ($\varphi = 7.9°$). This structural disposition allows the hydrogen atoms (H1 and H2) of the methyl group attached to the phenyl ring to form agostic interactions with the nickel atom, thus blocking the vacant coordination site of the catalyst. In addition to this, some conjugative effect between the first aryl ring and the Ni–diimine plane is expected to even further stabilize the cationic complex. The conformer **3a.II** also presents agostic interaction between the methyl group hydrogen atom and the nickel atom but, in this case, only one agostic interaction for the first aryl ring was observed. Conjugation effects are expected to be less evident in this conformer as the angle φ becomes larger (32.2°) in structure **3a.II**. Both conformers **3a.I** and **3a.II** present a partial blocking of the vacant site to monomer coordination, being more remarkable for **3a.I** (see Fig. 1). The conformer **3a.III** has the two aryl groups almost perpendicular to the diimine plane ($\varphi = 82.2°$ and $\varphi' = 83.6°$). In this case, the cationic species presents a less hindered vacant site accessible for ethylene coordination.

As mentioned above in the olefin polymerization mechanism [12,13], the ethylene coordination to Ni–diimine complex is the previous step to that of ethylene insertion into the metal–carbon bond. Therefore, these conformations should have a strong influence on the catalyst activity.

The relative energies for conformers **3a.I**, **3a.II** and **3a.III** are shown in Fig. 2. These numbers support the expected trends mentioned above. The conformer **3a.I** is the most stable one, 6.17 kcal mol^{-1} below **3a.II** and

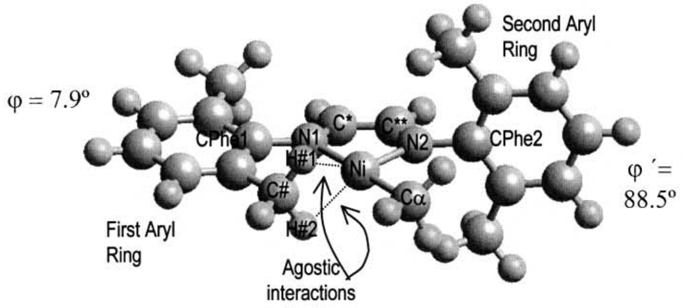

3a.I

Geometry parameters	
Ni-Cα	1.952
Ni-H#1	2.030
Ni-H#2	1.992
C#-H#1	1.121
C#-H#2	1.122
Ni-N1	2.010
Ni-N2	1.888
N1-C*	1.327
N2-C**	1.323
C*-C**	1.447
N1-CPhe1	1.420
N2-CPhe2	1.449
CPhe1-N1-Ni	121.5
CPhe2-N2-Ni	128.1
N2-Ni-Cα	95.4

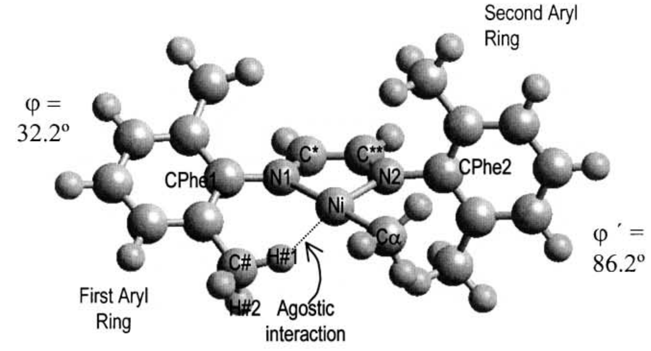

3a.II

Geometry parameters	
Ni-Cα	1.937
Ni-H#1	1.895
Ni-H#2	3.377
C#-H#1	1.119
C#-H#2	1.101
Ni-N1	2.005
Ni-N2	1.873
N1-C*	1.327
N2-C**	1.329
C*-C**	1.442
N1-CPhe1	1.418
N2-CPhe2	1.446
CPhe1-N1-Ni	124.2
CPhe2-N2-Ni	126.4
N2-Ni-Cα	96.3

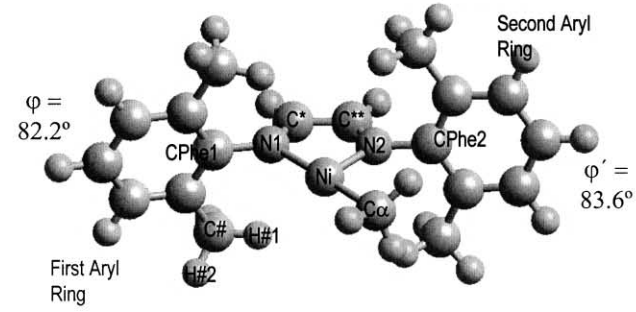

3a.III

Geometry parameters	
Ni-Cα	1.932
Ni-H#1	3.273
Ni-H#2	4.700
C#-H#1	1.099
C#-H#2	1.099
Ni-N1	1.983
Ni-N2	1.875
N1-C*	1.313
N2-C**	1.325
C*-C**	1.451
N1-CPhe1	1.440
N2-CPhe2	1.444
CPhe1-N1-Ni	123.8
CPhe2-N2-Ni	124.2
N2-Ni-Cα	98.4

Fig. 1. Optimized geometries calculated at the BP86/II level and nomenclature used for the **3a** system $[\{ArN{=}CH{-}HC{=}NAr\}NiCH_3]^+$. Distances and angles are in angstroms and degrees, respectively. The φ-angle definition is depicted in Scheme 2.

11.77 kcal mol^{-1} below **3a.III**. The formation of agostic interactions with the nickel atom and the conjugation between π clouds of the Ni–diimine ring and the aryl groups should account for the additional stabilization with respect to **3a.III**. On the other hand, **3a.I** and **3a.II** presents a less accessible coordination site for the ethylene to form the π-complex necessary for the monomer insertion step in the polymerization reaction. These facts provide an additional explanation to the lower activities experimentally found for the **3a** systems.

The energy profile and the evolution of φ angle for the ethylene approach to the cationic structures **3a.I** and **3a.II** are both displayed in Fig. 3. The reaction coordinate selected was the distance between the olefin midpoint and the nickel atom. When the ethylene approaches the nickel active site, it forces the rotation of the aryl group by increasing

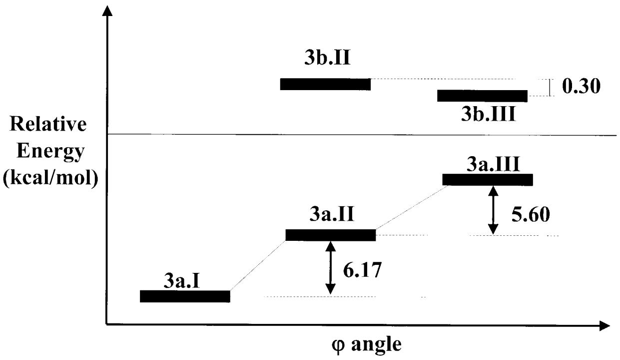

Fig. 2. Relative energies (kcal mol^{-1}) calculated at the B3LYP/LANL2DZ level on BP86-optimized geometries for the **3a** and **3b** systems.

the φ angle and finally going to a perpendicular conformation. As a result, it breaks up the agostic interactions and the delocalization of the π system (see Fig. 3a). Furthermore, energy barriers for ethylene uptake are observed for both **3a.I** and **3a.II** conformers (see Fig. 3b). As it would be expected, the energy cost for the π-complex formation with the **3a.I** conformer is higher than with the **3a.II** conformer (+17.56 versus +7.38 kcal mol^{-1}). Although it is not represented here, the ethylene π-complex with structure **3a.III** occurs without electronic energy barrier. The energy barrier of the ethylene insertion into the π-complex **3a** system was found to be 12.64 kcal mol^{-1}.

Taking into account the whole insertion reaction from resting state to resting state, the ethylene complexation step presents a higher energy barrier than ethylene insertion. Therefore, π-complex formation is expected to be the rate-limiting process in olefin polymerization with the **3a** catalysts, which have H atoms as substituents on the diimine ligand.

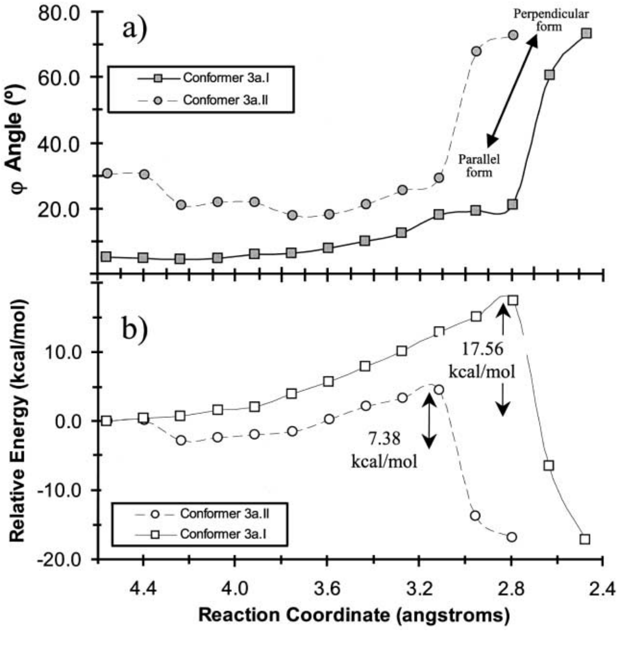

Fig. 3. (a) Energy profiles and (b) evolution of φ angles for the ethylene approaching to the cationic species **3a.I** (square + solid line) and the **3a.II** (circle + dashed line). The reaction coordinate corresponding to the distance between ethylene midpoint and nickel atom. Energy profiles were obtained by constraining the reaction coordinate in steps while optimizing all other coordinates. An additional constraint was used to restrict the ethylene approaching the catalyst along the equatorial plane.

On the other hand, for the complexes with the methyl groups attached to the diimine ligand (**3b** system, see Scheme 1), only two conformers (**3b.II** and **3b.III**) were found (see Fig. 4). Again the main difference observed concerns the φ angle. In this case, a conformer for **3b** similar to **3a.I** was not observed. The first aryl group cannot stand completely parallel to the diimine–Ni ring due to steric hindrance between the methyl groups attached to the diimine ring and the aryl ligands.

For this molecule, conformer **3b.III** is slightly more stable than conformer **3b.II** by 0.3 kcal mol^{-1} (see Fig. 2). Therefore, an energy barrier for the π-complex formation is hardly expected in this case. The insertion process itself would be responsible for the activation energy, being lower than the energy barriers obtained for ethylene coordination to the **3a** catalysts. This could provide an explanation for the higher activity experimentally found for the **3b** structures as compared to **3a** compounds (1800 kg of PE (mol Ni)$^{-1}$ h^{-1} for the **3b** systems versus 400 kg of PE (mol Ni)$^{-1}$ h^{-1} for the **3a** systems) [1].

4. Conclusions

In the present paper, we have studied the different conformations of the active catalyst species for two Brookhart's type catalysts (**3a** and **3b** systems). The relationship between these conformations and the catalyst activities has been suggested. The most important drawn conclusions are:

1. Three conformers for the active cationic species (**3a.I**, **3a.II** and **3a.III**) have been found for the **3a** catalyst, which differ in the relative position of aryl groups attached to the diimine ligand (φ angle in Fig. 1. Conformers **3a.I** and **3a.II** are found to be more stable than the conformer **3a.III**, due to agostic interactions and conjugative effects, which are responsible for this additional stabilization.
2. **3a.I** and **3a.II** conformers hinder the ethylene coordination to the nickel atom. Thus, the formation of the ethylene π-complex presents an energetic barrier, which in this case is higher than the ethylene insertion barrier itself. This could provide a plausible explanation for the lower activity experimentally found for ethylene polymerization with the **3a** catalyst as compared to the **3b** system.
3. For the **3b** system, which contains methyl groups attached to diimine ligand, the most stable conformer found corresponds to the structure named **3b.III**, where the two aryl rings lie perpendicular to the dimine plane. This geometrical disposition leaves the coordination site readily available

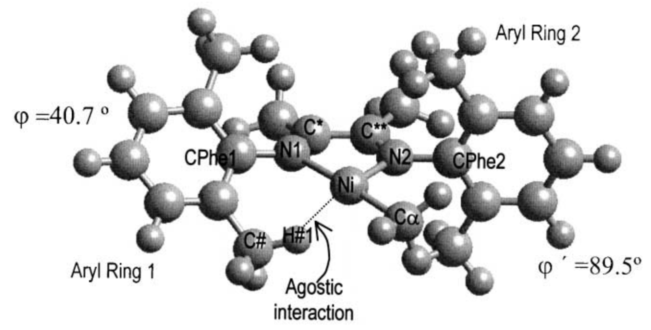

Geometry parameters	
Ni-Cα	1.936
Ni-H#1	1.914
C#-H#1	1.119
Ni-N1	1.988
Ni-N2	1.867
N1-C*	1.329
N2-C**	1.332
C*-C**	1.478
N1-CPhe1	1.430
N2-CPhe2	1.447
CPhe1-N1-Ni	122.2
CPhe2-N2-Ni	124.5
N2-Ni-Cα	97.5

3b.II

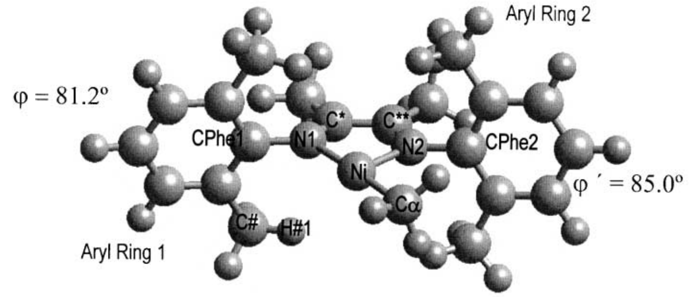

Geometry parameters	
Ni-Cα	1.932
Ni-H#1	3.296
C#-H#1	1.099
Ni-N1	1.974
Ni-N2	1.874
N1-C*	1317
N2-C**	1.331
C*-C**	1.480
N1-CPhe1	1.445
N2-CPhe2	1.447
CPhe1-N1-Ni	123.0
CPhe2-N2-Ni	123.4
N2-Ni-Cα	99.0

3b.III

Fig. 4. Optimized geometries calculated at the BP86/II level and nomenclature for the **3b** system $[\{ArN{=}CMe{-}MeC{=}NAr\}NiCH_3]^+$. Distances and angles are in angstroms and degrees, respectively.

for ethylene coordination, so the insertion barrier is expected to be the rate-limiting process for ethylene polymerization in this case.

Structures having bulky ligands attached to the diimine and capable of maintaining the aryl groups perpendicular to the Ni–diimine plane should be considered as firm candidates for the purpose of designing more active catalysts.

Acknowledgements

Thanks are due to the CICYT (Grant MAT99-1053) for the support of this investigation. One of us (J.R.) wishes to thank CICYT for the tenure of a fellowship. The authors also acknowledge Repsol-YPF for the permission to publish these data.

References

[1] Johnson LK, Killian CM, Brookhart M. J Am Chem Soc 1995;117:6414.
[2] Killian CM, Tempel DJ, Johnson LK, Brookhart M. J Am Chem Soc 1996;18:11664.
[3] Deng L, Margl PM, Ziegler T. J Am Chem Soc 1997;119:1094.
[4] Musaev DG, Froese RDJ, Svensson M, Morokuma K. J Am Chem Soc 1997;119:367.
[5] Musaev DG, Froese RDJ, Morokuma K. New J Chem 1997;21:1269.
[6] Strömberg S, Zetterberg K, Siegbahn PEM. J Chem Soc, Dalton Trans 1997;22:4147.
[7] Musaev DG, Morokuma K. Top Catal 1997;119:367.
[8] Deng L, Woo TK, Cavallo L, Margl PM, Ziegler T. J Am Chem Soc 1997;119:6177.
[9] Woo TK, Ziegler T. J Organomet Chem 1999;591:204.
[10] Froese RDJ, Musaev DG, Morokuma K. J Am Chem Soc 1998;120:1581.
[11] Musaev DG, Froese RDJ, Morokuma K. Organometallics 1998;17:1850.
[12] Arlman EJ, Cossee P. J Catal 1964;3:99.
[13] Brookhart M, Green MLH. J Organomet Chem 1983;250:395.
[14] ADF user's guide. ADF program system release. 1999.02.
[15] Vosko H, Wilk L, Nusair M. Can J Phys 1980;58:1200.
[16] Becke AD. Phys Rev A 1988;38:3098.
[17] Perdew JP. Phys Rev B 1986;33(12):8822.
[18] Frisch MJ, Trucks GW, Schlegel HB, Scuseria GE, Robb MA, Cheeseman JR, Zakrzewski VG, Montgomery JA, Stratmann RE, Burant JC, Dapprich S, Millan JM, Daniels AD, Kudin KN, Strain MC, Farkas O, Tomasi J, Barone V, Cossi M, Cammi R, Mennucci B, Pomelli C, Adamo C, Clifford S, Petersson GA, Ayala PY, Cui Q, Morokuma K, Malick DK, Rabuk AD, Raghavachari K, Foresman JB, Ciolowski J, Ortiz JV, Stefanov BB, Liu G, Liashenko A, Piskorz P, Komaromi I, Gomperts R, Martin RL, Fox DJ, Keith TA, Al-Laham MA, Peng CY, Nanayakkara A, Gonzalez C, Challacombe M, Gill PMW, Johnson BG, Chen W, Wong MW, Andres JL, Head-Gordon M, Reploge ES, Pople JA, GAUSSIAN 98 (Revision A.1). Pittsburgh (PA): Gaussian Inc. 1998.